Deuteron NMR study of liquid crystals confined in aerogel matrices

A. Zidanšek, S. Kralj, G. Lahajnar, and R. Blinc
J. Stefan Institute, University of Ljubljana, Jamova 39, 61111 Ljubljana, Slovenia
(Received 20 October 1994)

The temperature dependence of the deuteron NMR line shape was studied in pentylcyanobiphenyl (5CB) and octylcyanobiphenyl (8CB) liquid crystals confined in porous silica aerogel matrices with two different pore size distributions. The average pore sizes $\langle R_c \rangle$ of the two aerogel matrices were 0.8 and 0.2 μm, respectively. The deuteron NMR lines of 5CB and 8CB confined liquid crystals are in the isotropic regime broader than in the corresponding bulk phases. This observation shows that the interaction with the aerogel internal surface induces nematic order far above the bulk isotropic-nematic transition temperature. The nematic-isotropic (N-I) transition for both confined liquid crystals is continuous. No hysteresis was observed. A simple Landau-type model is used to describe these observations.

PACS number(s): 64.70.Md, 76.60.−k

I. INTRODUCTION

Liquid crystals are often referred to as "soft" systems [1] because of their relatively strong and spatially long ranged response to external disturbances. There are many experiments taking advantage of this peculiarity which effectively reveal many interesting properties of liquid crystals. Among the different phenomena investigated recently, finite size and surface effects are of particular interest. For such studies liquid crystals confined in cavities of different geometries are used.

Early studies have been limited to the cases where the geometry of the confining cavity is relatively simple (e.g., plane-parallel [2], spherically [3,4] or cylindrically [5] shaped cavities). More recently, studies have been extended to cavities of more complex geometry. In this respect, aerogel [6] porous matrices are of particular interest. Aerogels consist of a network of continuously connected voids of various shapes. The main advantages of an aerogel as a liquid crystal host are the following: (i) the porosity of aerogels is extremely high therefore providing host lattices of relatively high surface to volume ratio; (ii) the average void cavity dimension $\langle R_c \rangle$ can be in these systems far below 1 μm, where finite size effects become important. Here, R_c describes a typical void linear dimension and $\langle\ \rangle$ refers to an average over all cavities of the aerogel matrix. (iii) aerogels are transparent and, therefore, the structure of a confined liquid crystal can be also studied using optical spectroscopy in addition to magnetic resonance and other techniques.

There have been several recent experimental studies of liquid crystals confined into porous matrices. Aliev and Breganov [7] studied properties of 5CB nematic liquid crystals confined to porous glass matrices of average void size $\langle R_c \rangle \approx 100$ nm and $\langle R_c \rangle \approx 6.5$ nm, using dielectric spectroscopy and optical techniques. In their samples the nematic (N) to isotropic (I) phase transition is found to be gradual and the transition temperature $T_{NI}(\langle R_c \rangle)$ is apparently shifted to temperatures higher than in the bulk. They attributed this effect to the anchoring interaction W_a between the liquid crystal and void surfaces, and they estimated its magnitude as $W_a \approx 10^{-3}$ J/m^2. The N-I transition is accompanied by a strong thermal hysteresis. They claim this to be a consequence of surface induced smectic layers persisting over a distance of ≈ 10 nm into the cavity interior. Note that the bulk 5CB liquid crystal does not exhibit a smectic phase. The authors conjecture that smectic layers are induced by surface induced polarization. This effect should result from the relatively large dipole moment of the 5CB molecule.

Bellini *et al.* [8] studied properties of an 8CB liquid crystal embedded into an aerogel matrix using light scattering and precision calorimetry. Bulk 8CB exhibits in addition to a nematic also a smectic A (Sm-A) phase. The average void size was $\langle R_c \rangle \approx 20$ nm. They reached the following conclusions: (i) the N-I transition is under such severe confinement continuous; (ii) within experimental error the sample does not show any hysteresis behavior; (iii) the N-I transition temperature and nematic surface orientational order is depressed due to surface induced disorder; (iv) there is no evidence of a N–Sm-A transition. In the subsequent paper [9], the authors concentrated on the N–Sm-A phase transition. In order to probe the onset of smectic translational ordering with decreasing temperature, they used x-ray scattering. They show that confinement affects stronger the N–Sm-A transition than the N-I one. Within the temperature interval where the bulk Sm-A phase is stable, the smectic correlation length is below the characteristic cavity size. They suggest that the way in which smectic ordering grows depends on the type of Sm-A phase. Based on their observation, they suggest that (i) the investigated Sm-A phase is of type II (relatively prone to formation of defects compared to type I) and (ii) that the smectic ordering propagates from the cavity surface into the interior.

Wu, Goldburg, and Liu [10] performed quasielastic light scattering experiment on an 8CB liquid crystal confined to a silica gel matrix with an average pore size of $\langle R_c \rangle \approx 20$ nm. Their measurements showed that (i) the nematic-isotropic transition is gradual and displaced towards a lower temperature; (ii) no hysteresis behavior is

observed; (iii) the nematic domains span over several pore diameters; (iv) the dynamics of the order-parameter fluctuations in the nematiclike state is extremely slow and glasslike.

In [11] the behavior of a 5CB liquid crystal confined to aerogel matrices of typical cavity size $\langle R_c \rangle \approx 1$ μm with different aerogel pore surface treatments is studied. We used deuteron NMR and studied the NMR line shapes for nontreated and lecithin treated surfaces. The resulting spectra show a strong dependence on the surface preparation. From spectra obtained in the isotropic phase, we concluded that in all cases studied the aerogel porous surface enhanced nematic ordering. We estimated the anchoring strength $W_a^{(\mathrm{non})}$ of the nontreated surface as $W_a^{(\mathrm{non})} \approx 10^{-3}$ J/m^2 and of the lecithin treated surface as $W_a^{(\mathrm{lecithin})} \approx 10^{-4}$ J/m^2.

In this context it is also important to mention the work of Iannacchione *et al.* [12] on a similar system. They studied the deuteron NMR of a 5CB nematic liquid crystal confined to Vycor glass, which forms a random network of pores with an average radius $\langle R_c \rangle \approx 3.5$ nm. In contrast to the aerogel matrix, the Vycor glass pores' radii are of relatively uniform size and the pores are cylindrically shaped. The authors of Ref. [12] describe the continuous *N-I* transition with a simple model based on the Landau–de Gennes phenomenological approach.

Several authors have stressed the similarity between a nematic liquid crystal confined to an aerogel matrix and a system of magnetic spins in a random field. This analogy has been studied in detail by Maritan *et al.* [13]. They suggested two models, taking into account the head-to-tail invariance of nematic molecules. The predictions of a mean field theory have been supported by Monte Carlo simulations. Although their models are very simple they exhibit the essential phenomena observed experimentally. The results suggest the occurrence of a transition into a glasslike nematic phase without any hysteresis.

In this paper, we study deuteron NMR spectra of 5CB and 8CB liquid crystals confined in aerogel matrices of various pore size distributions. We use a simple model, similar to that suggested in Ref. [12], to reproduce the qualitative features of measured spectra. The paper is organized as follows. In Sec. II, we present the experimental setup. The description of our model is given in Sec. III with particular emphasis on the temperature shift and character of the *N-I* transition. The width of the deuteron NMR spectra is related to the parameters of our model. In Sec. IV, we present experimental results and analyze them using our model. In the last section, we summarize the obtained results.

II. EXPERIMENTAL SETUP

As a liquid crystal host, we use two aerogel matrices of different pore distributions. The pore size distribution was determined by mercury porosimetry and is given in Fig. 1. The average cavity size $\langle R_c \rangle$ of the two matrices is $\langle R_c \rangle \approx 0.8$ and 0.2 μm. In the following we refer to them as "micrometer"-size and "submicrometer"-size samples, respectively.

The initial step is preparing the aerogel is the sol-gel condensation in the acidic medium of a silicon alkoxide, tetraethoxysilane. In the "micrometer" sample a small amount of Cr^{3+} ions was added to the polymerization solution as an NMR relaxing agent for the purposes of another experiment [14]. The alkogel, which results from the gelation of this solution, consists of an interconnected network of branched polymers in which solvent molecules are embedded. An aerogel is obtained by evacuating the solvent from the alkogel under hypercritical con-

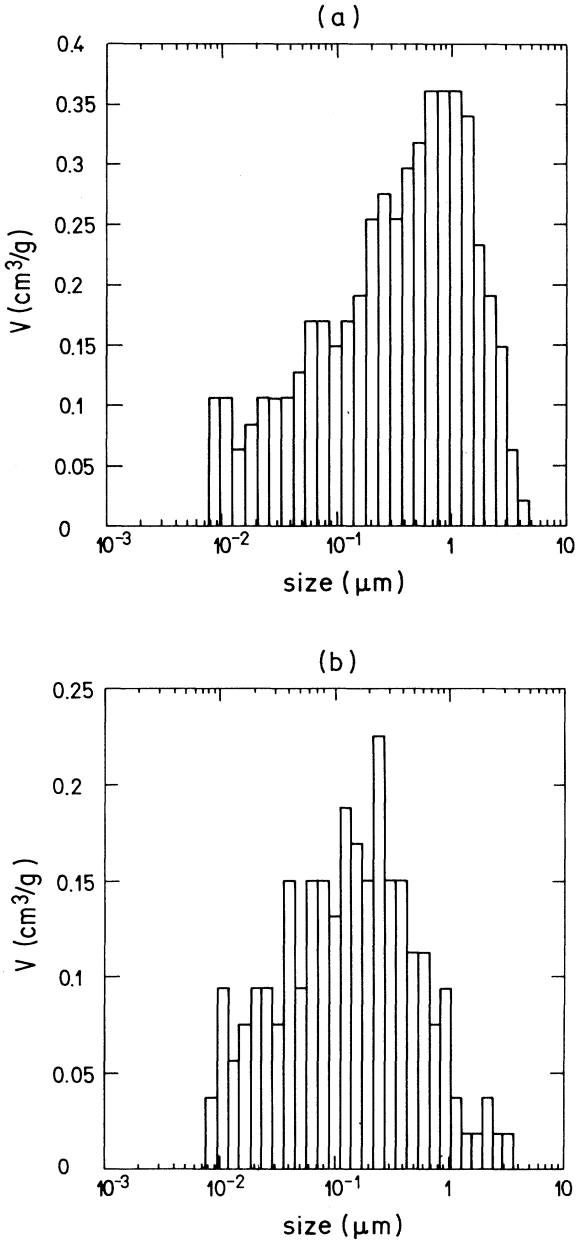

FIG. 1. Pore size distribution for the silica-aerogel sample as determined by mercury porosimetry: (a) "micrometer" and (b) "submicrometer" sample. The height of each column represents the pore volume per gram of aerogel for pores with sizes indicated on the horizontal axis.

ditions [6]. The information about the growth and structure of fractally rough silicate particles in solution can be found in the paper of Keefer and Schaefer [15]. The liquid crystal (8CB or 5CB) is introduced into the silica-aerogel matrix in the isotropic phase using capillary action.

The liquid crystal 5CB was deuterated at the βd_2 position, and the 8CB liquid crystal at the αd_2 position. Deuteron NMR spectra were recorded at a resonance frequency of 13.8 MHz, using a Bruker spectrometer with a variable-field iron magnet, as well as at 58.37 MHz using a wide bore 9 T superconducting magnet. A $(\pi/2)_x-(\pi/2)_y$ pulse sequence with phase cycling was used to obtain NMR spectra in the nematic and smectic phases. 512 to 8192 signal accumulations were taken in the low temperature nematic or smectic phase, and 128 averages in the high temperature isotropic phase.

III. THEORY

A. *N-I* transition in a cavity

In the following, we show qualitatively the effect of surface anchoring and elastic constants on the temperature shift and the character of the nematic-isotropic phase transition in a restricted geometry using a Landau-type potential. We confine ourselves to a nematic liquid crystal enclosed in a cavity of arbitrary shape with volume V and surface A. The nematic structure within the cavity is described with (i) the nematic director field $\vec{n}(\vec{r})$ pointing along the average local orientation of a nematic molecule at $\vec{r}$, and (ii) the nematic orientation order parameter $s(\vec{r})$ describing the amount of fluctuations about that direction. The free energy F_N of the nematic (N) phase is in our model given by [16–18]:

$$F_N=\int\left[a_0\frac{(T-T_*)}{T_*}s^2-bs^3+cs^4+f_e\right]dV+\int(-sW_a+s^2W_s)dA\ . \tag{1}$$

The first (volume) integral describes the bulk contribution. The quantities a_0, b, c are the Landau expansion coefficients, T is the temperature, T_* is the supercooling temperature of the nematic phase, and f_e is the nematic elastic energy. The second (surface) integral in Eq. (1) describes the influence of the nematic-cavity interface. The quantities W_a and W_s describe the strength of the surface interactions and depend on the orientation of nematic molecules at the interface . According to symmetry arguments [18] and predictions of microscopic theories [17,18], we allow the surface term to include a linear and a quadratic term in $s(\vec{r})$. The linear term $\propto -sW_a$ tends to increase the nematic orientational ordering at the surface. It originates from the interaction between the nematic molecules and the surrounding material. The quadratic term may result from the fact that molecules close to an interface have fewer nearest neighbors than in the bulk [17,18]. If this is the case, then this term tends to reduce the nematic ordering at the interface.

In this work we concentrate on the dependence of the average orientational order parameter on surface anchoring and elastic constants by neglecting details of orientational ordering. We replace the value of the local order parameter with its average value $\bar{s}_c$ in the cavity. We roughly approximate the elastic term in Eq. (1) by [12]

$$f_e\approx\frac{K\bar{s}_c^2}{2R_c^2}\ , \tag{1a}$$

where K stands for the average elastic constant and R_c describes a typical linear dimension of a cavity. Here we assume that director distortions typically extend over cavity size. Further, we discard orientational dependence of the surface terms W_a and W_s in Eq. (1).

B. Shift of the *N-I* transition temperature

At the nematic-isotropic transition $T=T_{NI}(R_c)$ we have $F_N=0$. When we replace the value of the local order parameter $s(\vec{r})$, with its average value $\bar{s}_c$, the condition $F_N=0$ transforms into

$$a_0\frac{[T_{NI}(R_c)-T_*]}{T_*}\bar{s}_c^2-b\bar{s}_c^3+c\bar{s}_c^4+\frac{K\bar{s}_c^2}{2R_c^2}+(-\bar{s}_cW_a+\bar{s}_c^2W_s)\kappa\approx 0\ . \tag{2}$$

This equation determines the temperature $T_{NI}(R_c)$ of the N-I transition and its dependence on R_c. The quantity $\kappa=A/V$ is the surface to volume ratio. In the bulk ($R_c\to\infty$) the transition takes place [19] at $T_{NI}\equiv T_{NI}(R_c=\infty)=T_*(b^2/(4ca_0)+1)$. In a cavity of a finite size our model yields for the N-I transition temperature shift $\Delta T=T_{NI}-T_{NI}(R_c)$:

$$\Delta T=\Delta T_e+\Delta T_a+\Delta T_s\ , \tag{3}$$

where

$$\frac{\Delta T_e}{T_*}=\frac{4c^2}{a_0b^2}\frac{K\bar{s}_c^2}{2R_c^2}\ , \tag{3a}$$

$$\frac{\Delta T_a}{T_*}=-\frac{4c^2}{a_0b^2}\bar{s}_cW_a\kappa\ , \tag{3b}$$

$$\frac{\Delta T_s}{T_*}=\frac{4c^2}{a_0b^2}\bar{s}_c^2W_s\kappa\ . \tag{3c}$$

The quantities ΔT_e, ΔT_a, ΔT_s describe the temperature shifts due to elastic distortions, anchoring interaction, and finite size effects, respectively. We see that elastic distortions always depress the transition temperature. A similar effect has the surface term described with W_s assuming $W_s>0$ as proposed from microscopic theory. The surface interaction term related to W_a shifts the N-I transition towards higher temperatures. To study the effect of the cavity size on the relative importance of the various terms in Eqs. (3), we approximate the surface to volume ratio with $\kappa\approx 1/R_c$ (for a spherical cavity $\kappa=3/R_c$). This suggests that $\Delta T_s\propto +1/R_c$, $\Delta T_a\propto -1/R_c$, $\Delta T_e\propto 1/R_c^2$ as already discussed by Aliev and Breganov [7]. In the case where the surface interac-

tion enhances nematic ordering it holds $|\Delta T_s| < |\Delta T_a|$. In relatively small cavities ΔT_e dominates because of its $1/R_c^2$ dependence.

C. Character of the *N-I* transition

We now study the dependence of the character of the *N-I* transition in a cavity of finite size on the surface anchoring and elastic constants. For this reason, we analyze the variation of $\bar{s}_c$ across the *N-I* transition. We start from the free energy density of the confined nematic liquid crystal, which is approximately

$$f_N \approx F_N/V \approx \left[a_0 \frac{(T-T_*)}{T_*} + \frac{K}{2R_c^2} + \frac{W_s}{R_c} \right] \bar{s}_c^2 - b\bar{s}_c^3 + c\bar{s}_c^4 - \frac{W_a \bar{s}_c}{R_c} . \quad (4)$$

The last term in Eq. (4) has a similar effect as an external field. Its presence induces a finite value of $\bar{s}_c$ even for $T > T_{NI}(R_c)$. The resulting phase is conventionally called the paranematic phase [2].

In order to simplify the calculations, we introduce dimensionless quantities [20],

$$q = \bar{s}_c 2c/b, \quad r = R_c/R_0, \quad t = \frac{4a_0 c}{b^2}\left[\frac{T-T_*}{T_*}\right], \quad \gamma = 2cK/(bR_0)^2, \quad \mu_a = 8c^2 W_a/(b^3 R_0), \quad \mu_s = 4cW_s/(b^2 R_0) . \quad (5)$$

Here μ_a, μ_s describe the dimensionless surface strength, γ is the renormalized elastic constant, t denotes the dimensionless temperature difference, and the linear dimensionless distance r is measured in units of $R_0 = 1$ μm, which is a characteristic size of our system. In this scaling, the dimensionless free energy $g = f_N 16c^3/b^4$ is expressed as

$$g = \left[t + \frac{\gamma}{r^2} + \frac{\mu_s}{r} \right] q^2 - 2q^3 + q^4 - \frac{\mu_a q}{r} . \quad (6)$$

The properties of a similar model are described in Ref. [21]. Here, we summarize the main features: (i) the dimensionless temperature t_{NI} of the *N-I* transition is given by

$$t_{NI} + \frac{\gamma}{r^2} + \frac{\mu_s}{r} = 1 , \quad (6a)$$

(ii) the *N-I* transition is discontinuous for $\mu_a/r < 0.5$ and continuous for $\mu_a/r \geq 0.5$. The variation of q for different field strengths $h = \mu_a/r$ as a function of $t_{\text{eff}} = t + (\gamma/r^2) + (\mu_s/r)$ is shown in Fig. 2.

D. The deuteron NMR spectrum

The deuteron NMR spectra $I(\nu)$ are known to be sensitive to orientational ordering and to the degree of motional narrowing, which is in our case mostly due to

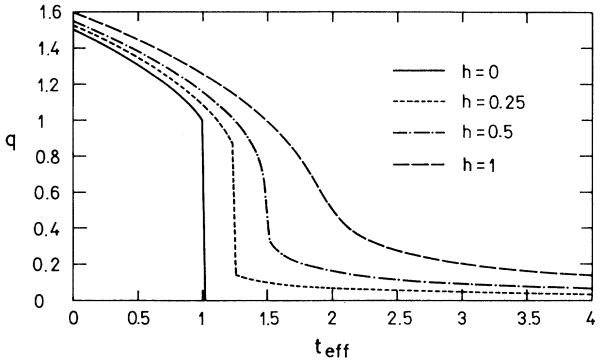

FIG. 2. The variation of the scaled nematic order parameter q as function of dimensionless effective temperature t_{eff} and field strength h.

the translationally induced rotation [22] (the so called TR mechanism) of liquid crystal molecules. The motional narrowing of $I(\nu)$ is pronounced if the director distortions are significant on a distance $d \approx \sqrt{D/(s_b \Delta\nu_0)}$ that a molecule migrates during the NMR measurement [22]. Here D stands for the average translational diffusion constant. The quantity $s_b \Delta\nu_0$ describes the static (with respect to the translational diffusion) line splitting of $I(\nu)$ in the bulk nematic phase and s_b describes a value of the nematic order parameter in the bulk nematic phase. In the nematic phase of an 8CB liquid crystal, we have $D \approx 10^{-11}$ m^{2}s^{-1}, $s_b \Delta\nu_0 \approx 40$ kHz so that $d \approx 100$ nm. More details about this effect are given in a previous paper [11].

In our model we express the deuteron NMR spectrum $I(\nu)$ of a confined deuterated liquid crystal as a sum of independent contributions of different cavities. Cavities are characterized by their typical size R_c. We express $I(\nu)$ as

$$I(\nu) = \sum_{R_c} I_c(\nu) P(R_c) , \quad (7)$$

$$I_c(\nu) = \frac{1}{N(R_c)} \sum_{i=1}^{N(R_c)} I_c^{(i)}(\nu) . \quad (7a)$$

Here 2ν describes the quadrupole splitting frequency. The sum $\sum_{R_c}$ runs over different values of R_c and $\sum_{i=1}^{N(R_c)}$ describes the sum over cavities with the same value of R_c. Thus $I_c^{(i)}(\nu)$ is a contribution of the ith cavity of the size R_c and $I_c(\nu)$ describes the contribution of all cavities of this size. The distribution of nematic molecules over cavities of different sizes is given by $P(R_c)$. The $P(R_c)$ dependence of our samples, measured by mercury porosimetry, is presented in Fig. 1.

In our model, we assume that the contribution $I_c(\nu)$ is powder shaped with a width [23]

$$\Delta\nu_c = m_c \bar{s}_c \Delta\nu_0 . \quad (8)$$

The quantity $\Delta\nu_0$ describes the splitting in the case of maximal ordering ($m_c = \bar{s}_c = 1$), and $\bar{s}_c$ is the average

orientational ordering within a cavity. The degree of motional narrowing in a cavity due to translational diffusion is given by m_c.

The assumption of a powderlike structure is based on the following reasoning. Let us describe by $\vec{N}_c^{(i)}=(\vec{n})$ the average director orientation in the ith cavity of the size R_c. In the case of $\vec{N}_c^{(i)}=0$ (i.e., in the case of an isotropic distribution of $\vec{n}$), the contribution $I_c^{(i)}(\nu)$ is powderlike and so is $I_c(\nu)$. But there is a large probability that $\vec{N}_c^{(i)}\neq 0$ in a cavity. In this case, we assume that the average of $\vec{N}_c^{(i)}$ over all cavities with the same R_c equals zero. This last conjecture is in agreement with the random character of the aerogel matrix. Therefore, also in this case, the contribution $I_c(\nu)$ is powder shaped. In addition, we assume that the external magnetic field **B** of the NMR experiment has negligible influence on orientational ordering of nematic molecules. The shape of the observed spectra justifies this approximation. We have measured NMR spectra for two different magnetic fields (2.1 and 9 T). Differences between the obtained spectra were negligible.

We thus assume that either the distribution of $\vec{n}$ in a cavity or the distribution of $\vec{N}_c^{(i)}$ over cavities with same R_c are isotropic. Note that the shape of $I_c(\nu)$ for $\vec{N}_c^{(i)}=0$ or $\vec{N}_c^{(i)}\neq 0$ can differ in the case of significant translational diffusion of nematic molecules within the NMR measurement time. The resulting motional averaging is more effective for $\vec{N}_c^{(i)}=0$ because in this case the director distortions are larger. In the following, we neglect this difference.

Taking into account the above assumptions, we define the effective width of $I(\nu)$ as

$$\langle \Delta\nu \rangle = \sum_{R_c} P(R_c)\Delta\nu_c = \Delta\nu_0 \sum_{R_c} P(R_c)\bar{s}_c m_c \ . \tag{9}$$

We obtain the value of $\bar{s}_c$ in a cavity via minimization of the free energy given by Eq. (4.4). The measured distribution $P(R_c)$ is given in Fig. 1.

IV. RESULTS AND DISCUSSION

We have measured the deuteron NMR spectra of 5CB and 8CB liquid crystals confined to silica-aerogel porous matrices for two different pore size distributions (the "micrometer" and "submicrometer" samples). In the isotropic phase of all the samples studied a single NMR line is observed, while the spectrum of the bulk nematic and smectic-A phases is a doublet. In Figs. 3(a), 3(b), the half-height widths are shown for the isotropic, nematic, and smectic phases for the confined samples, and for the isotropic phase of the bulk sample. The spectral splittings for the bulk samples in the nematic and smectic phases are also shown. A characteristic example of the temperature evolution of the NMR line shape for the confined liquid crystal is shown in Fig. 3(c). In the following, we analyze the spectra in the isotropic and nematic phases. In the case of 8CB, also, the region where the bulk liquid crystal exhibits the smectic-A phase is briefly discussed.

A. The isotropic phase

The absorption spectra in the isotropic phase of both silica-aerogel confined liquid crystals are broader by a factor of 1.5–2 than in the corresponding bulk isotropic phase. In addition, the spectra exhibit only a weak temperature dependence. This phenomena has been first observed by Crawford, Stannarius, and Doane [24] in a nematic liquid crystal confined to 0.2 μm cylindrical channels. They showed that this is due to the nematic-substrate interfacial interaction, which induces finite nematic orientational order s_0 within a surface layer. They attributed the observed weak temperature dependence of s_0 to surface interactions, which are local in nature. The thickness of the surface nematic layer is estimated to be comparable to a liquid crystal molecule length. Latter NMR investigations in cylindrical microcavities performed by Vrbančič *et al.* [25] revealed that such a behavior is characteristic for a system where nematic molecules strongly interact with the surface. In Ref. [25], a weak temperature dependence of s_0 above T_{NI} was observed for the case of tangential anchoring. In the case of homeotropic anchoring, on the other hand where the effective distance between the cylinder wall and the surface nematic molecules is larger as compared to the tangential case, a temperature variation was observed consistent with the predictions of the Landau-type theory.

On the basis of the results in the isotropic phase, we conclude that a nematic layer wets the silica-aerogel cavity surface before the bulk nematic transition is reached from above. Thus surfaces of aerogel cavities enhance nematic ordering. In addition, the weak temperature dependence of s_0 suggests that the nematic-surface interaction is relatively strong. This contrasts with the results obtained by Bellini *et al.* [8], and Clark *et al.* [9] in similar samples which find that the silica-aerogel surface tends to suppress nematic ordering in the nematic phase.

Several reasons can be responsible for this discrepancy. One possibility is that surface interactions tend to increase the nematic ordering, whereas the geometrical induced distortions oppose this tendency. To illustrate that let us assume that the aerogel surface is rough and has an undulated configuration with a typical wavelength λ and a similar amplitude. The state of the liquid crystal at the nematic-aerogel interface depends among others on the ratio [26] ξ_N/λ. Here, ξ_N denotes the nematic correlation length [16] describing a typical distance over which a locally disturbed nematic orientational order is recovered. If $\xi_N/\lambda > 1$ then it is energetically more favorable for a liquid crystal in the nematic phase to locally melt into the isotropic phase instead of forcing $\vec{n}(\vec{r})$ to follow strong undulations. Since λ is not temperature dependent the ratio ξ_N/λ has the same temperature behavior as ξ_N. Therefore, it is possible that $\xi_N/\lambda > 1$ in the nematic and $\xi_N/\lambda < 1$ in the isotropic phase. In this case, the orientational ordering is depressed in the nematic phase due to roughness of the surface although the surface interaction tends to increase $s(\vec{r})$. The other possible explanation is that different wetting properties of the aerogel surface are due to the competition of the surface

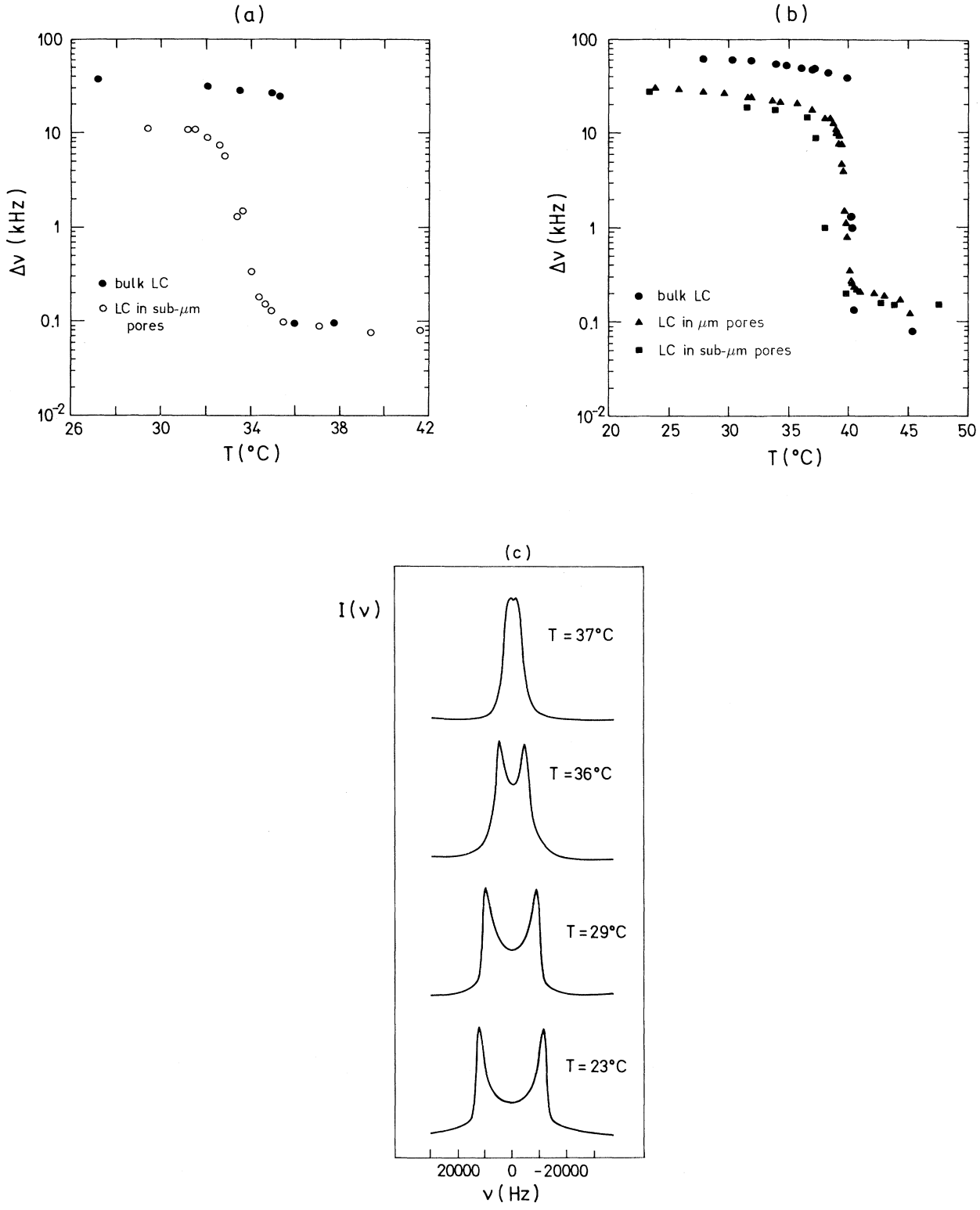

FIG. 3. The temperature dependence of the half-height width and spectral splitting $\langle \Delta\nu \rangle$ of the deuteron NMR absorption spectra of (a) 5CB deuterated at the βd_2 position and (b) 8CB deuterated at the αd_2 position. The half-height widths are shown for the isotropic, nematic, and smectic phases for the confined samples, and for the isotropic phase of the bulk sample. The spectral splittings for the bulk samples in the nematic and smectic phases are also shown. (c) The temperature evolution of the deuteron NMR spectrum of 8CB in the "submicrometer" aerogel matrix in the nematic and smectic A phases, showing the increase of the line splitting with decreasing temperature.

ordering term $+W_a s$ and the surface disordering term $-W_s s^2$, which are introduced in Eq. (1). Note that experimental data on reminiscent surfaces [18] suggest that this term is important. In principle, it could happen that the W_a term is dominant above T_{NI} and the W_s term below it. Another possibility is that this discrepancy occurs due to different typical pore sizes of our samples and those studied by Bellini, Clark *et al.* [8,9].

To estimate the surface induced ordering in the isotropic phase, we relate the line broadening with the degree of surface ordering s_0. The line splitting $\Delta\nu_{\rm iso}$ in the isotropic phase, broadened due to the finite surface ordering effect, can be approximately expressed as [27]

$$\Delta\nu_{\rm iso}\approx ds_0\Delta\nu_0\left[\frac{s_0\Delta\nu_0\pi}{D}\right]^{1/2}. \tag{10}$$

Here, d describes the thickness of the surface layer ($d\ll R_c$). In a derivation of (10), it is assumed that s_0 has a constant value within the surface layer and that $d\ll R_c$. In order to estimate s_0, we put $d\approx 4$ nm, $D\approx 10^{-11}$ m^{2}s^{-1}. For 8CB, we have $\Delta\nu_0\approx 100$ kHz, $\Delta\nu_{\rm iso}\approx 125$ Hz in the "micrometer" sample and $\Delta\nu_{\rm iso}\approx 155$ Hz in the "submicrometer" sample yielding $s_0\approx 0.015$ and $s_0\approx 0.017$, respectively. We conclude that the ordering tendency of the aerogel-liquid crystal interface increases with reduced $\langle R_c\rangle$.

B. Nematic phase

The *N-I* transition of the confined liquid crystals is gradual in all investigated samples. Within experimental error the measured spectra exhibit no hysteresis behavior. The gradual appearance of the *N-I* transition can either be a consequence of (i) the superposition of discontinuous temperature contributions of individual cavities of different $T_{NI}(R_c)$, or (ii) a consequence of relatively strongly weighted contribution from cavities in which the *N-I* transition is gradual.

In order to distinguish between these two cases, we compare the predictions of our model with the experimental results obtained in the 5CB [Fig. 4(a)] and 8CB [Fig. 4(b)] liquid crystal. In the calculation, we obtain $\bar{s}_c=qb/(2c)$ in each cavity via a minimization of Eq. (6). The line splitting of the whole sample is then evaluated using Eq. (9). The distribution $P(R_c)$ was taken from Fig. 1. The fit of the bulk spectrum, shown in Fig. 4, yields $b^2a_0/(4c^2T_*)\approx 0.2$ for both liquid crystals, $b/(2c)\Delta\nu_0\approx 36$ kHz in 8CB and $b/(2c)\Delta\nu_0\approx 23$ kHz in 5CB. Taking these parameters into account, we could best reproduce experimental results with our simple model for $\gamma\approx 0.002\pm 0.001$, $\mu_a<0.01$, $m_c\approx 0.95\pm 0.05$ for both "submicrometer" and "micrometer" sample as demonstrated in Fig. 4. In this calculation, we assume $\mu_a>\mu_s$ in accordance with the observed ordering effect in the isotropic phase. When evaluating the influence of motional narrowing, we simplified the calculation by assuming that in all cavities the value of m_c is comparable. We could not reproduce the relatively large temperature shift of T_{NI}. It is possible that this shift is a consequence of impurities introduced into the liquid crystal during the sample preparation. In order to fit experimental results for this case, we shifted the onset of ordering to $T_{NI}(R_c=\infty)$. Note that the discontinuous steps in Fig. 4 are consequences of the discrete $P(R_c)$ distribution used in calculations.

For the set of presented parameters, the contribution to $\Delta\nu$ of cavities where the *N-I* transition is continuous is negligible. This contribution becomes important for $\mu_a>0.01$ and relatively dramatically reduces the slope of the $q(t)$ curve in disagreement with experimental results. Thus, the analysis suggests that in both cases the observed gradual onset of nematic ordering is a consequence of temperature shifts induced by elastic distortions. The estimated value of $\mu_a\approx 0.01$ indicates that within our model, the continuous contribution comes from cavities whose sizes are less than ≈ 0.02 μm. This value is in agreement with experimental [3] and more detailed numerical [4,28] results of confined nematic liquid

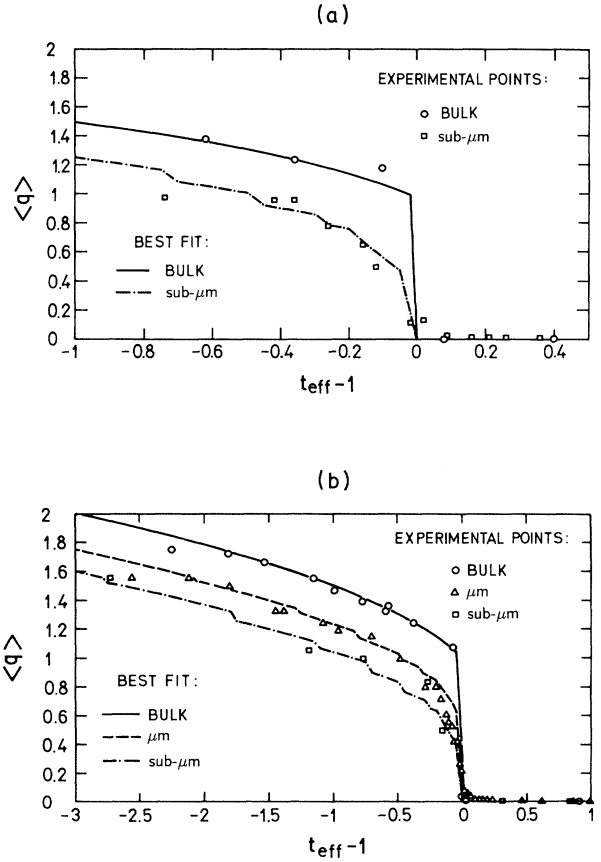

FIG. 4. The temperature dependence of the average scaled order parameter $\langle q\rangle=(2c/b)\Delta\nu/\Delta\nu_0$ of (a) 5CB and (b) 8CB liquid crystal for the bulk, "micrometer," and "submicrometer" samples. Full lines correspond to the best fit. The data in the bulk sample require $\Delta\nu_0 b/(2c)\approx 36$ kHz in 8CB, $\Delta\nu_0 b/(2c)\approx 23$ kHz in 5CB, and $b^2a_0/(4c^2T_*)\approx 0.2$ in both cases. In confined samples, we have in addition $\gamma=0.002$, $\mu_a=0.01$, $m_c=0.95$.

crystals in spherically shaped cavities. The estimated values for m_c, γ, and μ_a are reasonable. Taking into account typical values of liquid crystal material constants [19] and assuming $K \approx 10^{-11}$ N, $W_a \approx 10^{-4}$ J/m^2, we get $\gamma = 0.0005$, $\mu_a \approx 0.01$. The relatively large value of m_c indicates that the motional narrowing is not the dominant factor responsible for relatively slow temperature evolvement of the nematic order parameter.

C. The smectic phase

The bulk 8CB liquid crystal exhibits a second order transition into the Sm-A phase at [9] $T_{NA} \approx 306$ K. The Sm-A layered structure tends to orient nematic molecules along layer normals. This reduces the amount of director fluctuations and as a consequence the nematic order parameter is anomalously increased. This anomaly is relatively weak because the smectic order parameters are in 8CB only weakly coupled to the nematic order parameter. Therefore, to study the onset of Sm-A ordering the methods directly sensitive to layer formation are more adequate (e.g., x ray).

Our spectra do not reveal any apparent anomaly in the temperature range, where Sm-A ordering should appear. We believe that the temperature evolution of smectic ordering of a liquid crystal confined into a porous matrix is similar to the scenario proposed by Durand [26]. He studied the establishment of the Sm-A phase at a rough surface. He imitates the roughness with undulations of amplitude A_0 and spatial periodicity λ. His conjecture is that the liquid crystal state close to the surface depends crucially on the relative values of the smectic order parameter correlation length ξ_s, smectic twist, bend penetration lengths λ_t, λ_b, respectively, and the surface characteristic lengths A_0, λ. Here, ξ_s describes a typical distance over which a locally perturbed smectic translational order recovers. The penetration lengths estimate the distance over which the imposed twist or bend nematic director distortion persists in the bulk Sm-A phase. Note that in confined systems these characteristic distances have an upper boundary given by the typical cavity size if interactions among different cavities are negligible. According to this scenario just below the bulk Sm-A transition, where $\xi_s > A_0$, a region above the undulating surface remains nematic. With decreased temperature ξ_s is reduced. When $\xi_s \approx A_0$ the region of nematic ordering is either (i) limited to a surface layer of thickness $\approx \xi_s$ or (ii) limited to cores of disclinations, which are introduced to compromise the surface and Sm-A tendency. The scenario (i) is more probable for very rough surfaces ($A_0 \approx \lambda$) or/and Sm-A of type I (where $\xi_s > \lambda_t, \lambda_b$) and (ii) at smoother surfaces or/and Sm-A of type II (where $\xi_s < \lambda_t, \lambda_b$), which is more prone to defect formation. Still at a lower temperature where $\xi_s, \lambda_b, \lambda_t < A_0$ the nematic phase is limited only to the core of defects.

V. CONCLUSIONS

Deuteron NMR spectra of 5CB and 8CB liquid crystals confined to porous silica-aerogel matrices with two different pore size distributions have been studied as a function of temperature. The average pore size $\langle R_c \rangle$ of one aerogel matrix was 0.8 and 0.2 μm of the other one, respectively. The experimental data show a finite value of the average nematic order parameter $\langle s \rangle$ deep in the isotropic phase in both aerogel matrices. This reveals the ordering tendency of the aerogel surface, which enforces in aerogel pores a layer of 1 nm thickness having a finite nematic orientational order s_0 of 0.01. On decreasing temperature, the width of the NMR absorption line gradually increases on approaching the N-I transition. The temperature evolution of the nematic order parameter in the N-I transition region is different for the two aerogel matrices studied: the transition in the $\langle R_c \rangle = 0.8$ μm matrix starts at 313 K, which is ~ 2 K higher than in the $\langle R_c \rangle = 0.2$ μm matrix [see Fig. 3(b)]. Within experimental error no hysteresis behavior is observed.

A simple Landau-type model of the N-I transition has been developed to analyze the above experimental data. The aerogel sample is treated as an ensemble of independent cavities of different sizes. The elastic distortions within the cavities are roughly estimated. The average order parameter within a cavity $\bar{s}_c$ and its dependence on elastic properties and surface interaction strength—which in our model depend on the typical cavity size R_c—are also determined. The average sample order parameter $\langle s \rangle$ is then calculated taking into account the distribution of liquid crystal molecules per given cavity size $P(R_c)$. This quantity has been experimentally determined using mercury porosimetry. The analysis of experimental results with our model indicates that the gradual onset of nematic ordering is mainly due to the superposition of discontinuous N-I phase transitions in individual cavities. The contribution of small cavities in which the N-I transition is continuous is negligible.

The main drawback of our model is the rough estimate of elastic distortions, assuming a constant value of the orientational order parameter in a cavity and treating the system as being composed of independent cavities. Recent experimental data indicate that interactions between different pores are important [10,12] and that nematic domains can span over more than one cavity. Our preliminary calculations indicate that interactions between cavities tend to equalize the values of s in neighboring cavities. This would result in a sharpening of the peaks in the NMR absorption spectrum. A more detailed quantitative study would also have to take into account the spatial variation of $s(\vec{r})$. In this case, it would be convenient to treat the behavior of the system in terms of complete or partial orientational wetting [2,4,17,29,30]. But we believe that our model includes the essential qualitative features of the real sample.

[1] P. G. de Gennes, Science **265**, 495 (1992).
[2] P. Sheng, Phys. Rev. A **26**, 1610 (1982).
[3] A. Golemme, S. Žumer, D. W. Allender, and J. W. Doane, Phys. Rev. Lett. **61**, 2937 (1988).
[4] S. Kralj, S. Žumer, and D. W. Allender, Phys. Rev. A **43**, 2943 (1991).
[5] G. P. Crawford, D. W. Allender, J. W. Doane, M. Vilfan, and I. Vilfan, Phys. Rev. A **44**, 2570 (1991).
[6] J. Fricke, J. Non-Cryst. Solids **100**, 169 (1988).
[7] F. M. Aliev and M. N. Breganov, Zh. Eksp. Teor. Fiz. **95**, 122 (1989) [Sov. Phys. JETP **68**, 70 (1989)].
[8] T. Bellini, N. A. Clark, C. D. Muzny, L. Wu, C. W. Garland, D. W. Schaefer, and B. Olivier, Phys. Rev. Lett. **69**, 788 (1992).
[9] N. A. Clark, T. Bellini, R. M. Malzbender, B. N. Thomas, A. G. Rappaport, C. D. Muzny, D. W. Schaefer, and L. Hrubesh, Phys. Rev. Lett. **71**, 3505 (1993).
[10] X. Wu, W. I. Goldburg, and M. X. Liu, Phys. Rev. Lett. **69**, 470 (1992).
[11] S. Kralj, G. Lahajnar, A. Zidanšek, N. Vrbančič-Kopač, M. Vilfan, R. Blinc, and M. Kosec, Phys. Rev. E **48**, 340 (1993).
[12] G. S. Iannacchione, G. P. Crawford, S. Žumer, J. W. Doane, and D. Finotello, Phys. Rev. Lett. **71**, 2595 (1993).
[13] A. Maritan, M. Cieplak, T. Bellini, and J. R. Banavar, Phys. Rev. Lett. **72**, 4113 (1994).
[14] M. Chaput (private communication).
[15] K. D. Keefer and D. W. Schaefer, Phys. Rev. Lett. **56**, 2376 (1986).
[16] G. Vertogen and W. H. de Jeu, *Thermotropic Liquid Crystals* (Springer-Verlag, Berlin, 1988).
[17] A. Poniewierski and T. J. Sluckin, Liq. Cryst. **2**, 281 (1987).
[18] G. Barbero, E. Miraldi, and A. Stepanescu, J. Appl. Phys. **68**, 2063 (1990).
[19] E. B. Priestley, P. J. Wojtowitz, and P. Sheng, *Introduction to Liquid Crystals* (Plenum Press, New York and London, 1974), p. 143.
[20] N. Schopohl and T. J. Sluckin, J. Phys. **49**, 1097 (1988).
[21] D. J. Cleaver, S. Kralj, T. J. Sluckin, and M. P. Allen (unpublished).
[22] S. Žumer, S. Kralj, and M. Vilfan, J. Chem. Phys. **91**, 6411 (1989).
[23] A. Abragam, *The Principles of Nuclear Magnetism* (Clarendon Press, Oxford, 1962).
[24] G. P. Crawford, R. Stannarius, and J. W. Doane, Phys. Rev. A **44**, 2558 (1991).
[25] N. Vrbančič-Kopač, M. Vilfan, S. Žumer, G. P. Crawford, and J. W. Doane, in *The 15th International Liquid Crystal Conference Abstracts*, Proceedings of the 15th International Liquid Crystal Conference, Budapest, 1994, edited by L. Bata (Gordon and Breach, Langhorne, PA, 1994), Vol. I, p. 463.
[26] G. Durand, Liq. Cryst. **14**, 159 (1993).
[27] J. Dolinšek, O. Jarh, M. Vilfan, S. Žumer, R. Blinc, J. W. Doane, and G. P. Crawford, J. Chem. Phys. **95**, 2154 (1991).
[28] I. Vilfan, M. Vilfan, and S. Žumer, Phys. Rev. A **40**, 4724 (1990).
[29] P. Sheng, B.-Z. Li, M. Zhou, T. Moses, and Y. R. Shen, Phys. Rev. A **46**, 946 (1992).
[30] Y. L'vov, R. M. Hornreich, and D. W. Allender, Phys. Rev. E **48**, 1115 (1993).